Ordered Nanowell Arrays

Paul Pantano† and David R. Walt*

The Max Tishler Laboratory for Organic Chemistry, Department of Chemistry, Tufts University, Medford, Massachusetts 02155

Received June 10, 1996. Revised Manuscript Received August 16, 1996⊗

Ordered arrays of micrometer- and nanometer-sized wells were fabricated by chemically etching an optical imaging fiber's distal face. Well depth was controlled by the etch reaction time. Well packing densities could be increased by tapering the imaging fiber's distal tip. The smallest wells had a 50-nm depth and a 125-nm radius corresponding to a 3×10^{-18}-L volume and a packing density of 3.6×10^8 wells/cm^2. Ordered nanowell arrays were used as templates to emboss polymeric films with patterned nanometer-sized structures.

Introduction

The trend to develop two- and three-dimensional structures is converging on the nanometer scale. As a result, in addition to modern micromachining techniques such as electrochemical and chemical wet etching,[1−3] and dry etching[4,5] (whether or not used in combination with photolithographic techniques[6−8]), a variety of novel microfabrication techniques have evolved. For example, periodic particle array surfaces have been prepared by a lithographic procedure with masks comprising layer(s) of ∼250-nm-diameter polymer spheres;[9] patterned self-assembled monolayers of alkanethiolates, with features as small as a few hundred nanometers, have been formed by a "microcontact printing" approach;[10,11] a high-throughput imprint-lithographic method has produced metal patterns with 25-nm features;[12] and nanochannel array glass materials have been described and used as deposition masks to fabricate an array of ∼150-nm-diameter platinum dots on a silicon substrate.[13,14] In this work, we describe the characterization of ordered arrays of micrometer- and nanometer-sized wells fabricated on the distal face of an optical imaging fiber. In addition, we illustrate the array's potential as an embossing template for creating patterned polymeric films with nanometer-sized features.

Experimental Section

Array Fabrication. Micro- and nanowell array fabrication begins by successive polishing of the distal face of a 1000-μm diameter imaging fiber (Galileo ElectrOptics 1377-9955) with 30-, 15-, 3-, and 0.3-μm lapping films (General Fiber Optics, Fairfield, NJ). Residual polishing material was removed by sonicating the imaging fiber in water for 30 s. The imaging fiber's distal face was submerged at a right angle into a 700-μL solution comprising 100 μL of hydrofluoric acid (50%), 500 μL of ammonium fluoride (40%), and 100 μL of deionized water for a set period of time at room temperature.[15] **CAUTION: Hydrofluoric acid is extremely corrosive.** It is important to note that neither the overall diameter of the imaging fiber nor its planarity are compromised upon exposure to the etching solution. Finally, all imaging fibers were rinsed and sonicated thoroughly in water before analysis.

Tapered Imaging Fibers. An imaging fiber was tapered by simultaneously pulling and heating its distal tip with a standard glass capillary tube pipet puller (Narishige Model PE-2, Sea Cliff, NY). The final diameter of the tapered distal face was controlled by polishing. Specifically, after the tapered tip was potted in epoxy, the length of the imaging fiber's distal tip protruding from the polishing apparatus was adjusted to yield the desired final diameter.

Scanning Electron Microscopy. Scanning electron microscopy was performed with a JEOL SM 840 scanning electron microscope (Peabody, MA) at an operating voltage of 15 kV. Distal imaging-fiber faces were mounted on an aluminum stub and sputter coated with <10 nm of gold to minimize charging.

Atomic Force Microscopy. Contact-mode atomic force microscopy was performed with a Digital Instruments NanoScope IIIa (Santa Barbara, CA). In contrast to the scanning electron microscopic analyses, imaging fibers were not gold coated.

Results and Discussion

The template for the fabrication of micro- and nanowell arrays is an optical imaging fiber's distal face. A high-resolution imaging fiber comprises thousands of micrometer-sized, coherently fused optical fibers (i.e., the position of each optical fiber is the same at both the input and output ends). Imaging fibers are the main

† Present address: Department of Chemistry, University of Texas at Dallas, Richardson, TX 75083.

* To whom correspondence should be addressed. E-mail: DWalt@Pearl.Tufts.Edu.

⊗ Abstract published in *Advance ACS Abstracts,* October 1, 1996.

(1) Lee, H.-D.; Lee, H.-J.; Kim, C.-K.; Han, C.-H. *Appl. Phys. Lett.* **1995**, *66*, 3272−3274.
(2) Ottow, S.; Lehmann, V.; Foll, H. *J. Electrochem. Soc.* **1996**, *143*, 385−390.
(3) Datta, M. *J. Electrochem. Soc.* **1995**, *142*, 3801−3805.
(4) Ko, K. K.; Pang, S. W. *J. Electrochem. Soc.* **1995**, *142*, 3945−3949.
(5) Snider, G. L.; Then, A. M.; Soave, R. J.; Tasker, G. W. *J. Vac. Sci. Technol. B* **1994**, *12*, 3327−3331.
(6) Lochel, B.; Maciossek, A.; Quenzer, H. J. *J. Electrochem. Soc.* **1996**, *143*, 237−244.
(7) Christensen, C. P. *Med. Dev. Diagnostic Ind.* **1995**, *17*, 188−193.
(8) Kyung, J. H.; Lawandy, N. M. *Opt. Lett.* **1996**, *21*, 174−176.
(9) Hulteen, J. C.; Van Duyne, R. P. *J. Vac. Sci. Technol. A* **1995**, *13*, 1553−1558.
(10) Xia, Y.; Whitesides, G. M. *J. Am. Chem. Soc.* **1995**, *117*, 3274−3275.
(11) Xia, Y.; Kim, E.; Whitesides, G. M. *J. Electrochem. Soc.* **1996**, *143*, 1070−1079.
(12) Chou, S. Y.; Krauss, P. R.; Renstrom, P. J. *Science* **1996**, *272*, 85−87.
(13) Tonucci, R. J.; Justus, B. L.; Campillo, A. J.; Ford, C. E. *Science* **1992**, *258*, 783−785.
(14) Pearson, D. H.; Tonucci, R. J. *Science* **1995**, *270*, 68−70.
(15) Pangaribuan, T.; Yamada, K.; Jiang, S.; Ohsawa, H.; Ohtsu, M. *Jpn. J. Appl. Phys.* **1992**, *31*, L1302-L1304.

S0897-4756(96)00331-6 CCC: $12.00

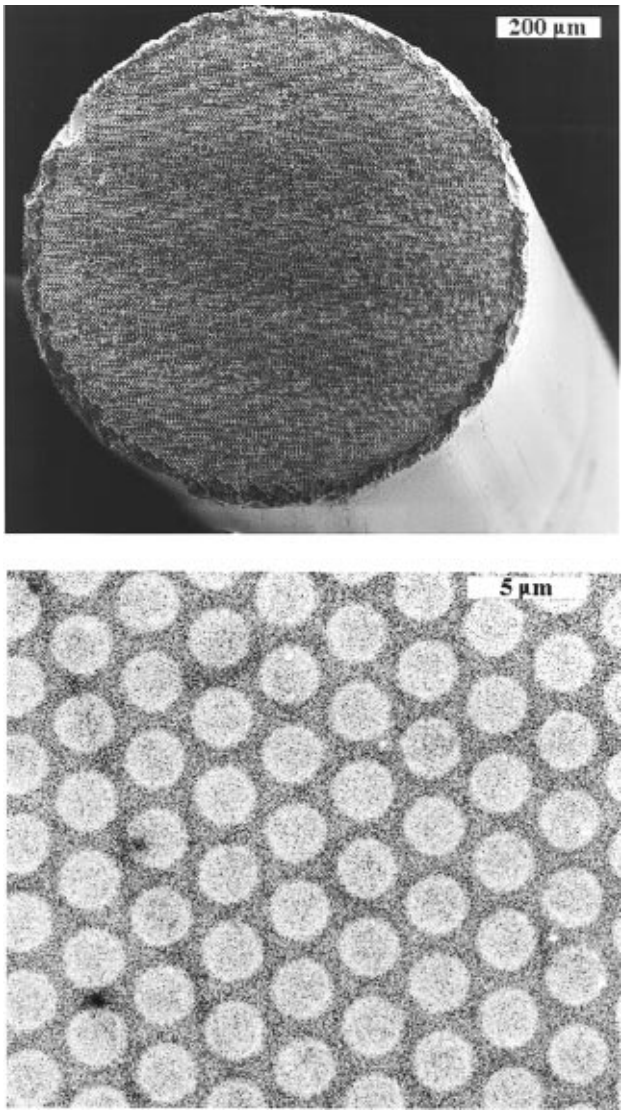

Figure 1. (A) Scanning electron micrograph of the distal face of a polished, chemically etched 1000-μm-diameter imaging fiber. (B) Scanning electron micrograph of the distal face of a polished, 1000-μm-diameter imaging fiber where the diameters of the individually cladded optical fiber cores (light regions) are $\sim$2.6 μm.

component of industrial or medical endoscopes where the size of the individual optical fibers determines the spatial resolution of a transmitted image.[16] The 1000-μm-diameter imaging fiber used in this work contains $\sim$70 000 individually cladded optical fibers (Figure 1A). Scanning electron microscopy shows that the diameter of each individual optical fiber core is $\sim$2.6 μm and that the packing density is $\sim 1 \times 10^7$ cores/cm^2 (Figure 1B). Wells are created at each core by a wet etching process. Selective core etching is achieved by exploiting the etchant's reactivity difference between the imaging fiber's high refractive index core and the low refractive index clad material. It is this differential etching rate that allows one to create unique architectures and structures. In brief, a polished imaging fiber's distal face is dipped into a buffered hydrofluoric acid solution for a fixed period of time. Figure 2A shows a scanning electron micrograph of a representative chemically etched, imaging fiber face that was treated with buffered

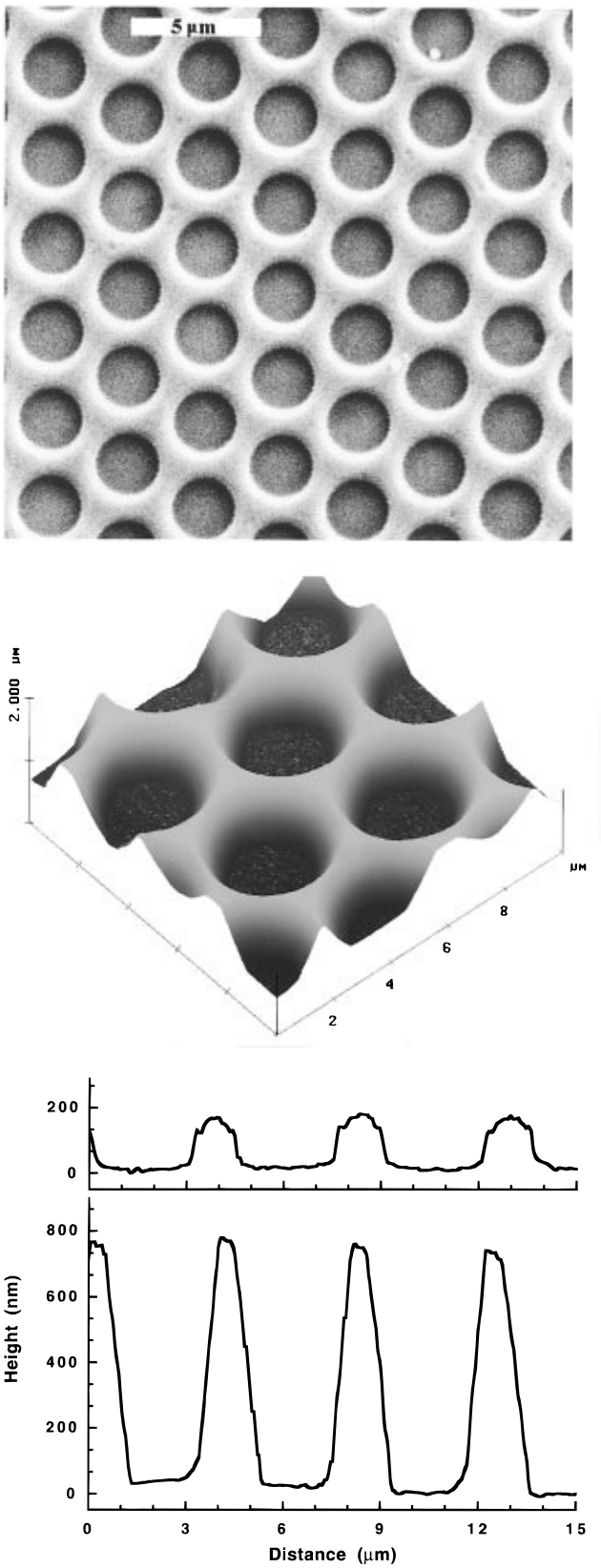

Figure 2. (A) Scanning electron micrograph of the distal face of a polished, chemically etched 1000-μm-diameter imaging fiber. (B) Atomic force micrograph of the distal face of a polished, 1000-μm-diameter imaging fiber that was chemically etched for 25 s. (C) Representative line profiles for an imaging fiber that was chemically etched for 15 s (top) and for an imaging fiber that was chemically etched for 60 s (bottom).

hydrofluoric acid solution for 30 s. The center-to-center spacing of the array of wells is 4.5 μm and the volume of each well is extremely small (e.g., the volume of a

(16) Pantano, P.; Walt, D. R. *Anal. Chem.* **1995**, *67*, 481A-487A.

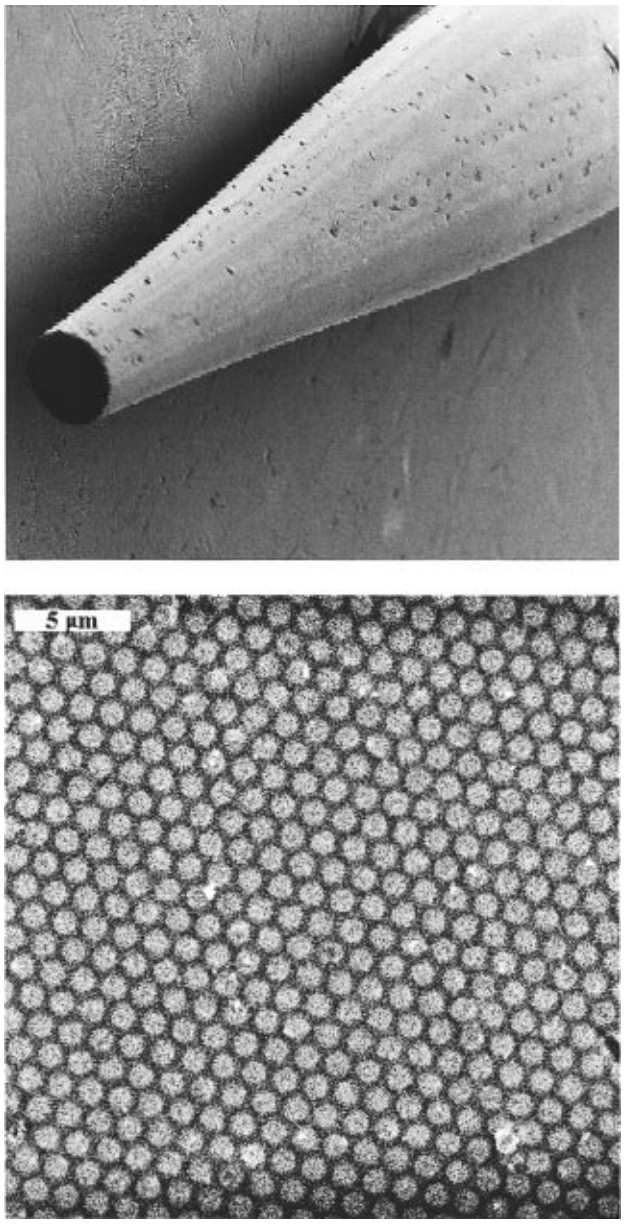

Figure 3. (A) Scanning electron micrograph of the distal tip of a polished, tapered imaging fiber where the diameter of the distal face is ~320 μm. (B) Scanning electron micrograph of the distal face of a polished, tapered imaging fiber (initial diameter ~1000 μm/final diameter ~325 μm) where the diameters of the individually cladded optical fiber cores (light regions) are ~0.85 μm.

300-nm deep well is ~2 fL (1 fL = 10^{-15} L)). Well depth and profiles were determined by atomic force microscopic analyses of the chemically etched imaging fiber face (Figure 2B,C). Well depth was proportional to etch time ($n = 4$; $r^2 = 0.9951$) at a rate of 24 nm/s for etch times less than 30 s. As shown in Figure 2C, well profiles depended upon the etch reaction time; qualitatively, a well's aspect ratio decreased with increasing etching times (i.e., with deeper well depths). Alternatively, a well's aspect ratio could be adjusted by controlling the etching solution's hydrofluoric acid-to-ammonium fluoride ratio.[15] Surprisingly, the smallest well depths were obtained by polishing alone (data not shown). Polishing these particular imaging fiber faces with 0.3-μm lapping film created an array of wells ~11−15-nm deep (presumably a result of the difference in hardness between core and clad glasses).

Table 1. Tapered Imaging Fiber Physical Dimensions

outer diameter imaging fiber (μm)	outer diameter individual cores (μm)	outer diameter ratio (imaging fiber/cores)
1000	2.6	385
325	0.85	382
175	0.48	365

Nanowell-array templates with smaller center-to-center spacings and higher packing densities could be obtained by tapering an imaging fiber's distal tip using a glass capillary pipet puller. Figure 3A shows a low magnification scanning electron micrograph of a polished, tapered imaging fiber's distal tip where the initial distal face diameter was 1000 μm and the final diameter of the tapered distal face is ~320 μm. Figure 3B shows a high magnification scanning electron micrograph of a polished, tapered imaging fiber's distal face where the diameter of the tapered face of the imaging fiber is ~325 μm and the packing density is ~6×10^7 cores/cm^2. Comparing the untapered (Figure 1B) and tapered (Figure 3B) imaging fiber's distal faces shows that the hexagonal packing architecture of the individually cladded optical fiber cores was not altered by the tapering process. Specifically, the core diameters at the center of the imaging fiber's distal face were identical to those at the periphery of the imaging fiber's distal face; presumably a result of the uniform heating of the imaging fiber by the pipet puller's heating filament. Furthermore, the diameters of both the tapered imaging fiber's distal face and its cores scaled precisely to the fiber's original dimensions ($n = 3$, $r^2 = 0.9998$; Table 1). This result is noteworthy because a ~500-nm-diameter core is 4−5 times smaller than the smallest cores found on commercially available (un)tapered imaging fibers, offering the possibility of enhancing the spatial resolution of endoscopic instrumentation.[17]

Tapered imaging fibers can also be etched. The atomic force micrograph and a representative line profile of a tapered, chemically etched imaging fiber are shown in Figure 4. This imaging fiber's distal face was tapered to produce an array of cores with ~250-nm center-to-center spacing and a packing density of 3.6×10^8 cores/cm^2. Subsequently, this imaging fiber's distal face was chemically etched to produce an array of 50-nm-deep wells where the volume of each individual well was 3 aL (1 aL = 10^{-18} L). Such wells may be suitable as micro- and nanoreaction vials for molecule trapping.

Ordered nanowell arrays were used as polymeric pattern-transfer templates. To illustrate this application, the distal face of the chemically etched imaging fiber shown in Figure 2B (where the original array of wells was 600-nm deep) was dipped into a siloxane copolymer solution and allowed to cure. The polymer solution comprised 0.3 g/mL Dow Corning 92-009 dispersion coating in toluene. The polymer cured upon solvent evaporation and the dip process was repeated five times. Figure 5 shows a polymeric film with a hexagonally packed array of 600-nm-tall polymeric cones obtained by peeling and inverting the polymer film off of the chemically etched imaging fiber. Since fused fiber-optic bundles and their individual optical fiber cores can be heated, tapered, and shaped into a variety of architectures and dimensions, the facile creation of a variety of polymeric patterns and struc-

(17) Shea, R. M. M.S. Thesis, Tufts University, 1996.

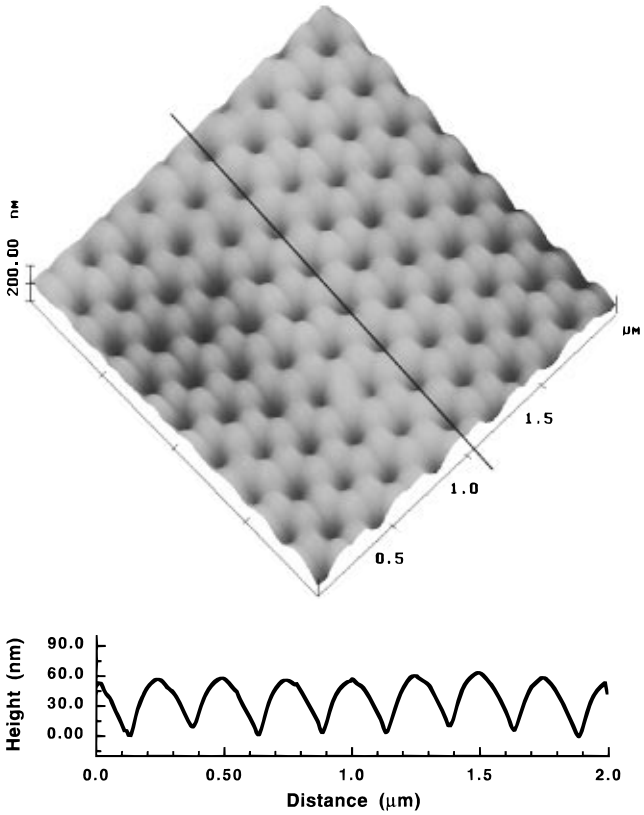

Figure 4. (A) Atomic force micrograph of the distal face of a polished, tapered imaging fiber (initial diameter ~1000 μm/final diameter ~52 μm) that was chemically etched for 2 s. (B) Cross-sectional analysis for the tapered, chemically etched imaging fiber shown above (see black line).

tures can be envisioned. In addition, reusable nanowell arrays and the polymeric pattern-transfer methodology could be used to fabricate microlens arrays,[18,19] embossable gratings,[20,21] or biosensor arrays.[22−24] The ultimate utility of this microfabrication methodology may arise by exploiting the fact that each well is connected to its own optical channel[25] allowing it to be addressed individually or as part of the entire imaging fiber array. Thus, after well fabrication, light could be employed to initiate additional processes such as deposition, polymerization, or ultraviolet curing to facilitate multistep operations that address complex microfabrication challenges.

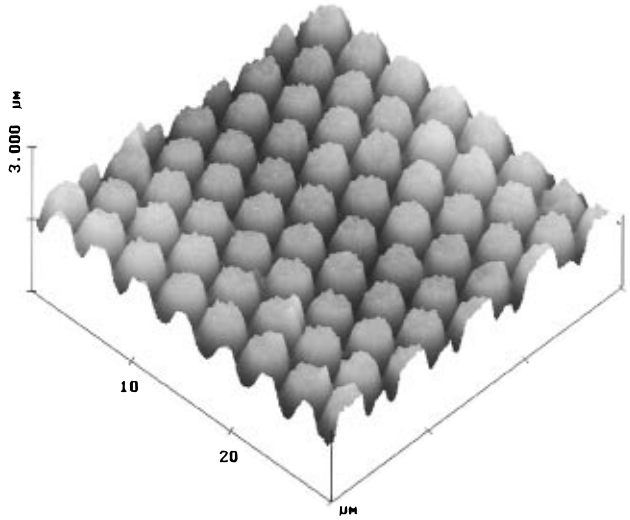

Figure 5. Atomic force micrograph of an inverted polymer layer after it was removed from the distal face of the polished, chemically etched 1000-μm-diameter imaging fiber shown in Figure 2B.

Acknowledgment. The authors gratefully acknowledge the National Institutes of Health (Grant GM 48142) and the Office of Naval Research (D.U.R.I.P. Award) for financial support, David A. McNally (Galileo ElectrOptics, Sturbridge, MA) for the imaging-fiber donation, and Professor John S. Kauer (Tufts Medical School, Boston, MA) for micropipet-puller usage.

CM9603314

(18) Kumar, A.; Abbott, N. L.; Kim, E.; Biebuyck, H. A.; Whitesides, G. M. *Acc. Chem. Res.* **1995**, *28*, 219−226.
(19) Beadie, G.; Lawandy, N. M. *Opt. Lett.* **1995**, *20*, 2153−2155.
(20) Roncone, R. L.; Weller-Brophy, L. A.; Weisenbach, L.; Zelinski, B. J. J. *J. Non-Cryst. Solids* **1991**, *128*, 111−117.
(21) Ramos, B. L.; Choquette, S. J.; Fell Jr., N. F. *Anal. Chem.* **1996**, *68*, 1245−1249.
(22) Pritchard, D. J.; Morgan, H.; Cooper, J. M. *Angew. Chem., Int. Ed. Engl.* **1995**, *34*, 91−93.
(23) Healey, B. G.; Walt, D. R. *Anal. Chem.* **1995**, *67*, 4471−4476.
(24) Li, L.; Walt, D. R. *Anal. Chem.* **1995**, *67*, 3746−3752.
(25) Healey, B. G.; Foran, S. E.; Walt, D. R. *Science* **1995**, *269*, 1078−1080.